Guanosine inhibits hepatitis C virus replication and increases indel frequencies, associated with altered intracellular nucleotide pools

Rosario Sabariegos[1,2,6¶], Ana M. Ortega-Prieto [4¶], Luis Díaz-Martínez [5], Ana Grande-Pérez [5], Isabel Gallego[4,7], Ana I. de Ávila[4], María Eugenia Soria[4,8], Pablo Gastaminza[7,9], Esteban Domingo,[4,6,7*,] Celia Perales[4,7,8*] and Antonio Mas[1,3,6*]

[1]Laboratorio de Virología Molecular, Centro Regional de Investigaciones Biomédicas (CRIB), Universidad de Castilla-La Mancha, Albacete 02008-Spain.

[2]Facultad de Medicina and [3]Facultad de Farmacia, Universidad de Castilla-La Mancha, Albacete 02008-Spain.

[4]Centro de Biología Molecular "Severo Ochoa", Consejo Superior de Investigaciones Científicas (CSIC)-Universidad Autónoma de Madrid (UAM), Campus de Cantoblanco, Madrid 28049-Spain.

[5]Instituto de Hortofruticultura Subtropical y Mediterránea "La Mayora," Consejo Superior de Investigaciones Científicas-Universidad de Málaga, Área de Genética, Facultad de Ciencias, Campus de Teatinos, Málaga, Spain.

[6]Unidad de Biomedicina UCLM-CSIC.

[7]Centro de Investigación Biomédica en Red de Enfermedades Hepáticas y Digestivas (CIBERehd) del Instituto de Salud Carlos III, 28029, Madrid, Spain

[8]Department of Clinical Microbiology, IIS-Fundación Jiménez Díaz, UAM. Av. Reyes Católicos 2, 28040 Madrid, Spain

[9]Department of Cellular and Molecular Biology, Centro Nacional de Biotecnología, Consejo Superior de Investigaciones Científicas (CSIC), Campus de Cantoblanco, Madrid 28049-Spain.

[¶]These authors contributed equally to this work.

*Corresponding authors: Antonio Mas

e-mail: Antonio.Mas@uclm.es

28 Celia Perales

29 e-mail: cperales@cbm.csic.es

30 Esteban Domingo

31 e-mail: edomingo@cbm.csic.es

Abstract

In the course of experiments aimed at deciphering the inhibition mechanism of mycophenolic acid and ribavirin in hepatitis C virus (HCV) infection, we observed an inhibitory effect of the nucleoside guanosine (Gua). Here, we report that Gua and not the other standard nucleosides inhibits HCV replication in human hepatoma cells. Gua did not directly inhibit the *in vitro* polymerase activity of NS5B, but it modified the intracellular levels of nucleoside di- and tri-phosphate (NDPs and NTPs), leading to deficient HCV RNA replication and reduction of infectious progeny virus production. Changes in the concentrations of NTP or NDP modified NS5B RNA polymerase activity *in vitro*, in particular *de novo* RNA synthesis and template switching. Furthermore, the Gua-mediated changes were associated with a significant increase in the number of indels in viral RNA, which may account for the reduction of the specific infectivity of the viral progeny, suggesting the presence of defective genomes. Thus, a proper NTP:NDP balance appears to be critical to ensure HCV polymerase fidelity and minimal production of defective genomes.

Author summary

Ribonucleoside metabolism is essential for replication of RNA viruses. In this article we describe the antiviral activity of the natural ribonucleoside guanosine (Gua). We demonstrate that hepatitis C virus (HCV) replication is inhibited in the presence of increasing concentrations of this ribonucleoside and that this inhibition does not occur as a consequence of a direct inhibition of HCV polymerase. Cells exposed to increasing concentrations of Gua show imbalances in the intracellular concentrations of nucleoside-diphosphates and triphosphates and as the virus is passaged in these cells, it accumulates mutations that reduce its infectivity and decimate its normal spreading capacity.

Introduction

Positive-sense single-stranded RNA viruses [(+)ssRNA viruses] are the most abundant pathogens for humans. The hepatitis C virus (HCV) is a hepacivirus that belongs to the *Flaviviridae* family of (+)ssRNA viruses. The HCV genome encodes information for the synthesis of ten proteins: core (C), envelope glycoproteins (E1 and E2), an ion channel (p7), NS2 protease, protease/helicase NS3 (and its cofactor NS4A), membrane-associated protein NS4B, regulator of viral replication NS5A, and RNA-dependent RNA-polymerase NS5B [1].

There are several ways to approach the control of RNA viral diseases. Inhibition of HCV functions by direct-acting antiviral agents (DAAs) has yielded sustained virological responses of about 98% [2,3]. Thus, HCV infection may be targeted for eradication by the combined use of different DAAs directed to viral proteins. However, access to this treatment is not affordable in countries with high prevalence rates, and an effective prophylactic vaccine is not available, making global HCV eradication difficult. Consequently, treatment with a combination of pegylated interferon-alpha (PEG-IFNα) plus ribavirin (Rib) is still in use in several countries with high prevalence rates of HCV infection [4].

Rib displays several mechanisms of antiviral activity [5], a major one being the inhibition of inosine-5'-monophosphate (IMP) dehydrogenase (IMPDH), which converts IMP to xanthosine monophosphate (XMP) and thus is involved in the *de novo* biosynthesis of GTP [6]. Rib also exerts its antiviral activity through lethal mutagenesis [7-10]. In the course of our experiments on the effect of mycophenolic acid and Rib on HCV clonal population HCV p0 [11] we observed that the presence of guanosine (Gua) during viral replication produced a decrease of up to 100 times in infectious progeny production. Although there are Gua derivatives that have antiviral properties, including Rib itself, natural Gua has never been identified as having antiviral activity [5]. The objective of the present study was to quantify the inhibitory role of Gua on HCV, its specificity, and its mechanism of action. We show that i) Gua inhibits infectious HCV progeny production but does not inhibit directly the HCV polymerase; ii) Gua alters the intracellular pools of di- and triphosphate ribonucleosides (NDP and NTP); iii) the

84 imbalance of the concentrations of NDP and NTP results in the inhibition of HCV polymerase
85 activity *in vitro*, and iv) Gua treatment is associated with an increase of indel frequency in
86 progeny HCV RNA. The results provide evidence of a metabolism-dependent mechanism of
87 generation of defective HCV genomes.

88

Results

Effect of ribonucleosides on HCV replication

Before studying the possible anti-HCV effect of natural nucleosides we determined their cytotoxicity (CC_{50}) on Huh-7.5 reporter cells. The cytotoxicity of Gua, adenosine (Ade), cytidine (Cyt) or uridine (Uri) was analyzed in semiconfluent cell monolayers by exposing cells to different nucleoside concentrations (from 0 µM to 800 µM). Cell viability (CC_{50}) was monitored after 72 h of treatment (Table 1) as described in Materials and Methods. Only Ade showed a modest cytotoxicity in the range of concentrations tested.

To quantify the inhibition of HCV infectious progeny production in the presence of nucleosides (IC_{50}), Huh-7.5 reporter cells were infected with HCV p0 at a multiplicity of infection (m.o.i.) of 0.05-0.1 $TCID_{50}$ per cell in the presence of increasing concentrations of the corresponding nucleoside, and infectious progeny production was measured as described in Materials and Methods. A decrease in the production of HCV infectious progeny was observed for Gua and Ade, whereas Cyt and Uri did not show any effect (Table 1). These data yield a therapeutic index (TI), defined as CC_{50}/IC_{50}, of 5.9 and $\geq$ 4.9 for Ade and Gua, respectively (Table 1).

To further explore the effect of ribonucleosides on HCV replication, HCV p0 was subjected to 5 serial passages in Huh-7.5 reporter cells, using an initial m.o.i. of 0.05 $TCID_{50}$ per cell, both in the absence and in the presence of ribonucleosides at 500 µM and 800 µM (Fig 1). Results show a consistent decrease in progeny infectivity as a result of Gua treatment (Fig 1A and 1B), but a sustained viral replication in the presence of Ade, Cyt or Uri (Fig 1C, D). In the presence of 500 µM Gua, a decrease in infectivity was detected although only one of the four replicates yielded values below the detection limit (Fig 1A). A sustained drop in HCV infectivity by Gua 800 µM was achieved, which became undetectable between passages 2 and 4 in all replicates (Fig 1B). Therefore, Gua was the only nucleoside that showed antiviral effect without cytotoxicity.

Next, we analyzed the effect of treatment with Gua, Ade, Cyt, and Uri in a surrogate single cycle infection model, taking advantage of spread-deficient bona fide HCV virions bearing a luciferase reporter gene (HCVtcp). This system recapitulates early stages of the infection

including viral entry, primary translation and genome replication, overall efficiency of which is proportional to reporter gene activity [12]. The results (Fig 2A) show that a selective HCV entry inhibitor, hydroxyzine, strongly interferes with reporter gene accumulation, as previously documented [13] (Figure 2A). Of the four natural nucleosides, only Gua exerted a significant inhibitory role, as shown by reduced luciferase levels in these cells (Figure 2A), and suggesting that an early step of the infection preceding viral assembly is significantly inhibited by Gua. To further dissect the impact of Gua on HCV replication, we analyzed the effect of Gua, Ade, Cyt and Uri treatment at different times in the replication of a dicistronic subgenomic genotype 2a (JFH-1) replicon bearing a luciferase reporter gene [12]. The objective was to analyze if the effect took place at the level of IRES-dependent translation (5 h post-transfection) or during RNA replication (24 and 48 h post-transfection) [13]. The results (Fig 2B) show that there are no differences among the different treatment points at 5 h post-transfection, which excludes an effect on HCV IRES-dependent RNA translation or any spurious interference with reporter gene expression. However, Gua-treated cells showed a statistically significant 12- and 5-fold reduction in RNA replication at 24 and 48 hours post-transfection respectively (Figure 2B). A modest (±2-fold) but significant reduction was also observed in Ade-treated cells. The fact that Ade treatment does not interfere with HCVtcp (trans-complemented HCV particles) infection suggests that only Gua affects significantly with HCV infection by interfering with viral RNA replication, downstream of viral entry and primary translation.

Effect of Gua on a high fitness HCV population

The HCV p100 virus [HCV p0 passaged 100 times in Huh-7.5 reporter cells], shows a relative fitness that is 2.2 times higher than that of the HCV p0 parental population [14]. Since viral fitness can influence the response of the virus to antiviral agents [15-17], HCV p100 was used to study the response of a high fitness HCV to Gua. For this, HCV p100 was subjected to 5 serial passages in Huh-7.5 reporter cells using an initial m.o.i. of 0.05 $TCID_{50}$ per cell, both in the absence and in the presence of Gua 500 or 800 μM. The results show a sustained drop in

143 infectivity of 15 and 736 times along the passages as a result of treatment with 500 and 800 μM
144 Gua, respectively. However, no decrease of infectivity below the limit of detection was
145 observed throughout the five passages in any of the replicates (Fig 1E). Only the decrease in
146 progeny production in the presence of 800 μM reached statistical significance (Fig 1E). Thus,
147 the results showed increased resistance of HCV p100 to Gua compared to HCV p0 (compare
148 Fig 1A, 1B, and 1E) as was previously observed with several antiviral drugs [16,17].

149

150 **Effect of Gua on the replication of other RNA viruses**

151 To determine the specificity of the antiviral action exerted by Gua on HCV and to rule out
152 nonspecific effects that could affect any virus, comparative experiments were conducted with
153 foot-and-mouth disease virus (FMDV), lymphocytic choriomeningitis virus (LCMV), and
154 vesicular stomatitis virus (VSV). First, the CC_{50} values of Gua, Ade, Cyt, and Uri were
155 determined for BHK-21 cells, as described in Materials and Methods. The values obtained
156 (Table 2) indicate no detectable cytotoxicity of Gua, Cyt and Uri, and a CC_{50} value of 391 ± 68
157 μM for Ade. To determine the IC_{50} values of these nucleosides, BHK-21 cells were infected
158 with FMDV, LCMV, and VSV, at an initial m.o.i. of 0.05 $TCDI_{50}$ per cell in the presence of
159 increased nucleoside concentrations and the production of infectious progeny was measured.
160 The values obtained (Table 2) show that all nucleosides lacked inhibitory profile for FMDV. In
161 contrast, purines were inhibitory for VSV, while all nucleosides were inhibitory for LCMV.
162 However, the IC_{50} values were very high and the therapeutic indexes (TI) were consequently
163 low (Table 2).

164 As an additional control for the specificity of HCV inhibition by Gua, the response of VSV,
165 FMDV and LCMV to nucleoside treatment in serial infections was studied. BHK-21 cells were
166 infected with FMDV, LCMV, and VSV with an initial m.o.i. of 0.05 $TCDI_{50}$ per cell, and were
167 subjected to 3 passages both in the absence and presence of nucleosides at a final concentration
168 of 800 μM. The analysis of the viral populations in passage 3 showed no statistically significant
169 difference from the viral titer obtained in the absence of treatment (Fig 3A-C). Therefore, the

results show that the only differences found were those of HCV treatment with Gua at 800 μM (Fig 1A-B). Finally, to rule out that the inhibitory effect of Gua on HCV was solely due to the action of the nucleoside on the human hepatoma cells used in the experiments, we examined the production of VSV viral progeny in Huh-7.5 reporter cells which this virus also productively infects. High viral titers in the presence of 800 μM Gua were obtained for VSV, confirming a lack of antiviral activity of Gua against this virus also in Huh-7.5 reporter cells (Fig 3D).

Effect of guanosine on HCV NS5B activity

To analyze the mechanism by which Gua inhibits HCV replication we tested the effect of increasing Gua concentrations on HCV polymerase activity *in vitro*. A 570 nt RNA fragment corresponding to the E1/E2 region of the HCV genome [18] was replicated by HCV recombinant NS5BΔ21 in the presence of ATP, CTP, GTP, and UTP, and at increasing concentrations of Gua (Fig 4A). NS5B polymerase activity increased with Gua concentration up to 500 μM. Even at 1 mM Gua, the RNA polymerase activity was similar to that obtained in absence of Gua. Only at very high Gua concentration (10 mM) the RNA polymerase activity showed a significant reduction (Fig 4A). Similar results were obtained using the 19-mer oligonucleotide LE19 (Fig 4B). Therefore, according to this *in vitro* RNA synthesis assay, the inhibition of HCV progeny production by Gua cannot be attributed to direct inhibition of the HCV RNA polymerase.

Effect of guanosine on intracellular nucleotide pools

To investigate whether HCV replication inhibition by Gua could be related to alterations in di- and triphosphate ribonucleoside intracellular concentrations, the level of NTPs and NDPs in Huh-7.5 reporter cells was determined in the absence of Gua and after 72 h of treatment with 500 or 800 μM Gua. Intracellular nucleoside triphosphate concentrations did not change when the cells were treated with 500 μM Gua. However, 800 μM Gua treatment resulted in a

196 statistically significant 2-fold increase (range from 2- to 2.2-fold) in intracellular concentration
197 of all NTPs (Fig 5A). In the case of NDPs a significant increase of 1.7- to 4.1-fold was observed
198 in cells treated with 500 μM Gua (Fig 5B). Treatment with 800 μM Gua resulted in an increase
199 of the concentration (2.1- to 5.4-fold) of all NDP's (Fig 5B). Therefore, the presence of Gua in
200 the culture medium increased the intracellular levels of nucleoside di- and tri-phosphates
201 (Supplementary Table). The lowest nucleotide concentration was obtained for CDP and CTP
202 independently of the treatment with Gua.

203

204 **Effect of nucleoside di- and triphosphate imbalance on HCV NS5B activity *in vitro***

205 To explore if changes in nucleotide concentrations might affect HCV polymerase activity, we
206 performed *in vitro* RNA polymerization experiments with recombinant NS5BΔ21 in the
207 presence of increasing concentrations of NTPs or NDPs. CTP and CDP were not included in the
208 analyses because they showed small intracellular variations (Supplementary Table) and CTP
209 was chosen as the carrier of the radioisotope. *De novo* (DN), primer extension (PE) and
210 template switching (TS) polymerase activities were measured in the presence of increasing
211 concentrations of the corresponding triphosphate nucleosides (Fig 6). A high UTP concentration
212 of 1 mM slightly but significantly decreased primer extension activity (Fig 6A). However, the
213 main effect of NTP concentration was on the *de novo* RNA synthesis, with a significant
214 decrease at high ATP concentration (Fig 6B), and a significant increase at high GTP
215 concentration (Fig 6C). The increase in the *de novo* RNA synthesis was accompanied by an
216 increase of template switching (Fig 6C).

217 Since increasing concentrations of Gua also altered the intracellular NDP concentrations (Fig 5),
218 we investigated if the presence of increasing concentration of NDPs might affect the NS5B
219 RNA polymerase activity *in vitro*. DN, PE, TS activities were measured in the presence of
220 increasing concentrations of the corresponding diphosphate nucleosides at a fixed nucleoside-
221 triphosphate concentration (Fig 7). The main effect of the presence of NDP was on the *de novo*

RNA synthesis, with a significant decrease at high ADP and GDP concentrations. Differences in primer extension and template switching did not reach statistical significance (Fig 7).

Mutational effects of guanosine

To determine if Gua-related nucleotide pool effects were associated with the mutation repertoire exhibited by HCV during replication in Huh-7.5 cells, the mutant spectrum of the genomic region spanning the last 49 nucleotides of the NS4B gene and the first 490 nucleotides of the NS5A gene, was analyzed using molecular cloning and Sanger sequencing. Following three passages in absence or presence of Gua, the maximum mutation frequency resulted in a significant increase in the HCV populations passaged in the presence of Gua ($p<0.0001$ and $p=0.01$ for Gua 500 μM, and Gua 800 μM, respectively; χ^2 test) (Table 3). A hallmark of virus extinction by lethal mutagenesis is the decrease of specific infectivity (the ratio between viral infectivity and the amount of genomic viral RNA) [7]. Extinction by Gua occurred with a 2.8-fold to 11.8-fold decrease of specific infectivity in the first two passages in the presence of the compared drug, as quantified by infectivity and viral RNA in samples of the cell culture supernatants (Fig 8), suggesting that an increase in polymerase error rate was involved. The most remarkable change was that replication in the presence of Gua increased significantly the number of indels in the heteropolymeric genomic regions of the mutant spectrum (Table 4). Indels in homopolymeric regions ─consisting of at least three successive identical nucleotides─ were not considered because control experiments revealed that they can be amplification artifacts [19]. No indels were detected in the 53 molecular clones derived from the population passaged in the absence of Gua. In sharp contrast, 10 deletions and 2 insertions were present in the 64 molecular clones retrieved from the population passaged in the presence of 500 μM Gua, and 5 deletions in 68 molecular clones from the population passaged in the presence of 800 μM Gua (Table 4). The difference in the number of deletions is highly significant for the populations passaged in the presence of 500 μM and 800 μM Gua ($p<0.001$; test $\chi 2$). The size of the deletions ranged from 1 to 46 nucleotides, some were found in a single clone, others in

several clones, and none of the deletions and insertions were in phase; they all generated a premature STOP codon (Table 4 and Fig 9). Therefore, the anti-HCV effect of Gua, exerted via nucleotide-mediated alterations of polymerase activity, is associated with the generation of multiple deletions during HCV replication.

Discussion

Nucleoside derivatives are the most important family of drugs targeting viral polymerases, but the antiviral capacity of natural nucleosides has not been described [5]. Interestingly, we observed an inhibitory effect of Gua when it was used in experiments to analyze the impact of mycophenolic acid and ribavirin on HCV progeny production [11]. Here, we document inhibition of HCV replication by Gua in single and serial infections of Huh-7.5 cells that led to loss of infectivity without significant toxicity for the host cells. The antiviral action of Gua was also exerted on high fitness HCV, albeit without loss of infectivity after 5 passages in the presence of Gua, in agreement with the drug resistance phenotype displayed by high fitness HCV (Fig 1) [14-17]. The antiviral effect of Gua was not observed for FMDV in BHK-21 cells or for LCMV and VSV in Huh-7.5 cells (Fig 3).

RNA synthesis by NS5BΔ21 was not significantly affected by Gua concentrations up to 1 mM. Therefore, the inhibition of virus progeny production is unlikely to be the result of direct polymerase inhibition by Gua. This result is consistent with previous work that showed the ability of NS5B to initiate RNA synthesis with this nucleoside [20]. In contrast to Gua, altered intracellular nucleotide concentrations affected the activity of NS5B, in particular an alteration of the *de novo* RNA synthesis by the GTP/GDP and/or ATP/ADP balances (Fig 7). The NS5B protein has an allosteric binding site of GTP and the balance between NDP and NTP might modulate RNA synthesis through this site [21-23].

Some GTP-dependent proteins play a role in the HCV replication cycle. They include proteins involved in virus entry into the cells (i.e HRas), proteins involved in translation (i.e.the eIF5B factor), or in replication (i.e. GBF1) [24-26]. The GTP-dependent Rab18 protein, which is located in the lipid droplets, is involved in capturing proteins such as viral protein NS5A into the replication complex [27]. The observed increase in GTP concentration in Gua-treated cells would not adversely affect the functionality of these proteins.

Some antiviral drugs exert their activity through alterations in the intracellular nucleotide pools [6,28]. Treatment of Huh-7.5 reporter cells with Gua produced an overall increase of

intracellular nucleoside di- and tri-phosphate concentrations (Fig 5). An increase of ATP would be beneficial for virus replication as ATP increments have been associated with the formation of the HCV replication complex [29]. Using previously reported cell volume values for HepG2 cell line (20) (ranging from 2.54 pL to 2.96 pL), the intracellular ATP concentration in Gua-treated Huh7.5-reporter cells would be in the range of 2 mM (Supplementary Table), similar to the previously described values in the HCV replication sites [29].

Intracellular concentration of mono- and di-phosphate nucleotides also modulates metabolic pathways critical for virus replication. For example, HCV proteins NS4B and NS5A inhibit the cellular protein AMP-activated protein kinase (AMPK) [30]. Inhibition of AMPK induces the synthesis of fatty acids and cholesterol that are of vital importance in the HCV replication sites. ADP activates AMPK [31,32], and the inactivation of AMPK by NS4B and NS5A is ineffective when ADP is increased [30]. As a result, there is no longer accumulation of fatty acids and cholesterol, and viral replication stops. Metformin activates AMPK by increasing AMP and ADP, and this effect has been associated with inhibition of HCV replication. [31,33,34]. The AMPK dissociation constant for ADP is in the range of 1.3-1.5 μM [32]. Therefore, the increase of the ADP concentration from 40 μM to 200 μM (Fig 4 and Supplementary Table) could be preventing, at least in part, inactivation of AMPK. Whether ATP acts only as a substrate or it also exerts some regulatory role needs to be further analyzed.

Defective viral genomes are increasingly recognized as players in virus-host interactions (reviewed in [35]). They are associated with multiple types of genetic lesions ranging from point mutations to large deletions. Deletions can result from polymerase slippage over one or several nucleotides, but the environmental factors that may trigger their occurrence are unknown. Generation of RNA deletions has been documented during *in vitro* replicase copying of viral RNAs [36], and deletions have been observed in many viruses [35,37-40]. Template switching is considered as the primary mechanism of copy-choice recombination of poliovirus in cells [41], and the primary mechanism of poly(rU) RNA synthesis by poliovirus polymerase [42]. The observed increase of indels in the presence of high GTP concentrations may be linked

310 to the enhanced template switching observed with the HCV polymerase *in vitro*. Despite limited
311 information on the origin of HCV defective genomes, there is solid evidence of the implication
312 of defective viral genomes in the interference with replication of their standard infectious
313 counterparts [43], including a contribution to viral extinction by lethal mutagenesis [44,45].
314 They also play a role as stimulators of antiviral responses [46], and as mediators of virus
315 attenuation and persistence [40,47,48], among other functions [35].
316 Defective genomes have been described for HCV, including in-frame deletion mutants. They
317 are present in patient plasma, exosomes and liver biopsies and they may play regulatory roles
318 during viral replication [49-53]. Little is known about the molecular mechanisms of generation
319 of defective genomes despite detailed accounts of their high m.o.i.-dependent selection based on
320 molecular complementation with standard genomes [35]. Our results provide evidence of a
321 mechanism of generation of defective HCV genomes fuelled by nucleoside pool effects on HCV
322 polymerase activity. This is accompanied by a significant reduction of the specific infectivity of
323 the passaged viral pools, demonstrating the increasing presence of non-infectious viral genomes
324 in the supernatants of Gua-treated cells. In addition to unveiling a possible mechanism of
325 generation of defective HCV genomes, our results open the possibility that the alteration of
326 cellular metabolic pathways may be a complementary strategy to the action of antiviral agents
327 to produce reductions in viral load and promote the extinction of HCV.
328

Material and methods.

Reagents and plasmids.

Nucleosides Ade, Cyt, Gua, and Uri, as well as nucleoside di- and tri-phosphates were purchased from Sigma-Aldrich. Plasmid pNS5BΔ21 encoding the HCV NS5B that lacks the C-terminal 21 hydrophobic amino acids to enhance solubility has been described previously [54]. The resulting expression vector allows the expression of a tagged NS5BΔ21 with six histidine residues at its C terminus to aid in protein purification.

Cells and viruses.

The origin of Huh 7.5, Huh 7-Lunet, Huh-7.5 reporter cell lines and procedures used for cell growth in Dulbecco's modification of Eagle's medium (DMEM), have been described [11]. Cell lines were incubated at 37°C and 5% CO_2. We used the following viruses in the experiments: HCV p0, obtained from HCVcc [Jc1FLAG2(p7-nsGluc2A)] (genotype 2a) and GNN [GNNFLAG2(p7-nsGluc2A)] (a replication-defective virus with a mutation in the NS5B RNA-dependent RNA polymerase) [11,55]. Mock-infected cells maintained in parallel with the infected cultures were prepared to control the absence of contaminations; no infectivity in the mock-infected cultures was identified in the experiments.

Trans-encapsidated HCV virions (HCVtcp) were produced by electroporation into packaging cells of a subgenomic, dicistronic HCV replicon bearing a luciferase gene, as previously described [12]. Supernatants of the electroporated cells were titrated to determine the optimal dose rendering detectable luciferase activity at 48 hours post-inoculation. The same subgenomic replicon was used for lipofection experiments, using lipofectamine2000 transfection reagent as previously described [13].

Production of viral progeny and titration of infectivity.

The procedures used to obtain the initial virus HCV p0 and for serial infections of the hepatoma Huh-7.5 reporter cells have been described [14]. Briefly, electroporation of Huh-7 Lunet cells

was performed with 10 µg of the transcript of HCVcc (Jc1 or the negative control GNN) (260 volts, 950 µF). Then, electroporated cells were passaged every 3–4 days before cells became confluent; passages were continued until 30 days post-electroporation. Subsequently, the cell culture supernatants were pooled to concentrate the virus 20 times using 10,000 MWCO spin columns (Millipore), and aliquots were stored at −70°C [14]. For titration of HCV infectivity, cell culture supernatants were serially diluted and applied to Huh-7.5 cells. After 3 days post-infection the cell monolayers were washed with PBS, fixed with ice-cold methanol, and stained with anti-NS5A monoclonal antibody 9E10 [14].

Toxicity test and inhibitory concentration.

The CC_{50} was calculated by seeding 96-well plates with Huh-7.5 cells and exposing them to the compound under study during 72 hours. MTT [3-(4,5-dimethylthiazol-2-yl)-2,5-diphenyltetrazolium bromide] was added at 500 µg/ml; after 4 h crystals were dissolved with 100 µl of DMSO and the O.D. measured at 550 nm; 50% cytotoxicity was calculated from quadruplicate determinations [11].

IC_{50} values were calculated relative to the controls without treatment (defined as 100% infectivity) [56]. Determinations were performed in triplicate.

RNA extraction, cDNA synthesis, PCR amplification, and nucleotide sequencing.

Intracellular RNA was obtained from infected cells using the Qiagen RNeasy kit (Qiagen, Valencia, CA, USA). RNA from cell lysates or cell culture supernatants was extracted using the Qiagen QIAamp viral RNA mini kit (Qiagen, Valencia, CA, USA). Reverse transcription (RT) of different HCV genomic regions was performed using avian myeloblastosis virus (AMV) reverse transcriptase (Promega), and subsequent PCR amplification was carried out using AccuScript (Agilent Technologies), with specific primers. Primers for the HCV amplification and the sequencing have been described [11,14,17,19]. Agarose gel electrophoresis was used to analyze the amplification products, using HindIII-digested Φ-29 DNA as a molecular mass standard. In parallel, mixtures without template RNA were reverse transcribed and amplified to monitor the absence of cross-contamination by template nucleic acids. Nucleotide sequences of

HCV RNA were determined on the two strands of the cDNA copies [11,55]; only mutations detected in the two strands were considered. To analyze the complexity of mutant spectra by molecular cloning and Sanger sequencing, HCV RNA was extracted and subjected to RT-PCR to amplify the NS5A-coding regions, as has been previously described [11]. Amplifications with template preparations diluted 1:10 and 1:100 were performed to ensure that an excess of template in the amplifications was used in the mutant spectrum analysis; the molecular cloning was performed from the undiluted template only when the 1:100-diluted template produced also a DNA band; this procedure avoids complexity biases due to redundant amplifications of the same initial RNA templates [11]. Control analyses to confirm that mutation frequencies were not affected by the basal error rate during amplification have been previously described [57]. Amplified DNA was ligated to the vector pGEM-T (Amersham) and used to transform *Escherichia coli* DH5α; individual colonies were taken for PCR amplification and nucleotide sequencing, as previously described [56].

NDP and NTP pool analysis.

The procedure used has been previously described [11]. Briefly, Huh-7.5 cells (2×10^6 cells) were washed with PBS and incubated with 900 µl of 0.6 M trichloroacetic acid on ice for 10 min. A precooled mixture of 180 µl of Tri-n-octylamine (Sigma) and 720 µl of Uvasol® (1,1,2-trichlorotrifluoroethane, Sigma) was added to the 900 µl extract, vortexed for 10 s, centrifuged 30 s at 12,000 × g at 4 °C, and stored at −80 °C prior to analysis. One hundred µl samples were applied to a Partisil 10 SAX analytical column (4.6 mm×250 mm) (Whatman) with a Partisil 10 SAX guard cartridge column (4.6×30 mm) (Capital HPLC) using an Alliance 2695 HPLC system connected to a 2996 photodiode array detector (Waters). NDP and NTP were separated at a eluent flow rate of 0.8 ml/min and detected with ultraviolet light at a wavelength of 254 nm. The column was pre-equilibrated with 60 ml of 7 mM $NH_4H_2PO_4$, pH 3.8 (buffer A). The separation program started with 22.5 min of an isocratic period with buffer A, continued with a linear gradient of 112.5 min to the high concentration buffer 250 mM $NH_4H_2PO_4$, 500 mM KCl, pH 4.5 (buffer B) and ended with an isocratic period of 37.5 min with buffer B. A processing

method was done using the Waters Empower™ Chromatography Data Software. To this end, 50 µl of 20 pmol/µl UTP, CTP, ATP and GTP (Jena Bioscience), were separated prior to sample analysis. The HPLC analysis did not separate rNTPs from dNTPs, or rNDPs from dNDPs. However, since the absolute concentration of rNTPs and rNDPs is several orders of magnitude greater than that of dNTPs dNDPs, we consider the value obtained as the concentration of rNTPs and rNDPs. Determinations were carried out with two independent biological samples, each one in triplicate for NDPs and NTPs. The amount of each nucleoside in cell extracts was normalized relative to the number of cells.

Quantification of HCV RNA.

Real time quantitative RT-PCR was performed with the Light Cycler RNA Master SYBR Green I kit (Roche), following the manufacturer's instructions, as previously described [14]. The 5′-UTR non-coding region of the HCV genome was amplified using as primers oligonucleotide HCV-5UTR-F2 (5′- TGAGGAACTACTGTCTTCACGCAGAAAG; sense orientation; the 5′ nucleotide corresponds to HCV genomic residue 47), and oligonucleotide HCV-5UTR-R2 (5′-TGCTCATGGTGCACGGTCTACGAG; antisense orientation; the 5′ nucleotide corresponds to HCV genomic residue 347). Quantification was relative to a standard curve obtained with known amounts of HCV RNA, obtained by *in vitro* transcription of plasmid GNN DNA [55]. Reaction specificity was monitored by determining the denaturation curve of the amplified DNAs. Mixture without template RNA and RNA from mock-infected cells were run in parallel to ascertain absence of contamination with undesired templates.

NS5BΔ21 polymerase expression and purification.

NS5B from strain pJ4-HC with a deletion of 21 aa at the C-terminal end (NS5BΔ21) was obtained as previously described [54,58]. This truncated protein displays polymerase activities that were not distinguished from those of the full-length enzyme [59]. Briefly, NS5BΔ21 was overexpressed in BL21DE3 Rosetta bacteria by IPTG induction and purified by affinity chromatography in a Ni-NTA column. Aliquots of the purest and most concentrated protein samples were adjusted to 50% glycerol and stored at -80°C until use. All purification processes

were monitored by SDS-PAGE and Coomassie brilliant blue staining. Protein was quantified by SDS-PAGE gel imaging and protein determination using the Bradford assay.

In vitro RdRP replication assays.

RNA polymerase assays were carried out using two different RNA substrates, the symmetric substrate LE-19 (sequence 5' UGUUAUAAUAAUUGUAUAC 3'), which is capable of primer-extension (PE), *de novo* initiation (DN), and template switching (TS) [54,58], and an RNA fragment encompassing HCV E1/E2 region (570 nt) [18]. Except when indicated otherwise, template RNA was pre-incubated for 15 minutes in a reaction mixture containing 20 mM MOPS, pH 7.3, 35 mM NaCl, 5 mM $MnCl_2$, 100 nM NS5B and GTP at the indicated concentration for each experiment. Reactions were started by adding 1 µCi of $\alpha[^{32}P]$CTP (3000 Ci mmol, PerkinElmer Life Sciences) and nucleoside-triphosphate as indicated in each experiment. When appropriate, reactions were performed in the presence of increasing concentrations of nucleotide diphosphates. Reactions were carried out in a final volume of 10 µl, at room temperature for 30 minutes, and stopped using EDTA/formamide loading buffer. E1/E2 products were resolved using 1% agarose gel electrophoresis. Agarose gels were dried in an electrophoresis gel dryer (BioRad). LE19 products were resolved using denaturing polyacrylamide (23% PAA, 7 M urea) gel electrophoresis. Gels were exposed to phosphorimager screens and scanned with a Typhoon 9600 phosphorimager (Molecular Dynamics). Sample quantification was performed from parallel experiments. Band volume values were obtained by using the ImageQuant software provided with the apparatus (GE Healthcare).

Statistical analyses.

The statistical significance of differences between mutation frequencies was evaluated by the chi-square test. Statistical comparisons among groups were performed with Student's T-tests. Unless indicated otherwise, the statistical significance is indicated by asterisks: * $p<0.05$; ** $p<0.005$; *** $p<0.0005$.

Acknowledgements.

C.P. is supported by the Miguel Servet program of the Instituto de Salud Carlos III (CP14/00121) cofinanced by the European Regional Development Fund (ERDF). CIBERehd (Centro de Investigación en Red de Enfermedades Hepáticas y Digestivas) is funded by Instituto de Salud Carlos III. The work at CBMSO was supported by grants SAF2014-52400-R from Ministerio de Economía y Competitividad (MINECO), SAF2017-87846-R, BFU2017-91384-EXP from Ministerio de Ciencia, Innovación y Universidades (MICIU), PI18/00210 from Instituto de Salud Carlos III, S2013/ABI-2906, (PLATESA from Comunidad de Madrid/FEDER) and S2018/BAA-4370 (PLATESA2 from Comunidad de Madrid/FEDER). The team at CBMSO belongs to the Global Virus Network (GVN). The work in Albacete was supported by grants SAF2016-80451-P, EQC2018-004420-P, and EQC2018-004631-P from MICIU, and by Plan Propio of the University of Castilla-La Mancha. The work in Malaga was supported by Plan Propio of the University of Málaga. Institutional grants from the Fundación Ramón Areces and Banco Santander to the CBMSO are also acknowledged. Piet de Groot is acknowledged for critical reading the manuscript.

References.

1. Scheel TK, Rice CM (2013) Understanding the hepatitis C virus life cycle paves the way for highly effective therapies. Nat Med 19: 837-849.
2. European Association for the Study of the Liver. Electronic address eee, European Association for the Study of the L (2018) EASL Recommendations on Treatment of Hepatitis C 2018. J Hepatol 69: 461-511.
3. Lombardi A, Mondelli MU, Hepatitis ESGfV (2019) Hepatitis C: Is eradication possible? Liver Int 39: 416-426.
4. Hlaing NK, Banerjee D, Mitrani R, Arker SH, Win KS, et al. (2016) Hepatitis C virus therapy with peg-interferon and ribavirin in Myanmar: A resource-constrained country. World J Gastroenterol 22: 9613-9622.
5. De Clercq E, Li G (2016) Approved Antiviral Drugs over the Past 50 Years. Clin Microbiol Rev 29: 695-747.
6. Wray SK, Gilbert BE, Noall MW, Knight V (1985) Mode of action of ribavirin: effect of nucleotide pool alterations on influenza virus ribonucleoprotein synthesis. Antiviral Res 5: 29-37.
7. Perales C, Gallego I, de Avila AI, Soria ME, Gregori J, et al. (2019) The increasing impact of lethal mutagenesis of viruses. Future Med Chem 11: 1645-1657.
8. Asahina Y, Izumi N, Enomoto N, Uchihara M, Kurosaki M, et al. (2005) Mutagenic effects of ribavirin and response to interferon/ribavirin combination therapy in chronic hepatitis C. J Hepatol 43: 623-629.
9. Cuevas JM, Gonzalez-Candelas F, Moya A, Sanjuan R (2009) Effect of ribavirin on the mutation rate and spectrum of hepatitis C virus in vivo. J Virol 83: 5760-5764.
10. Dietz J, Schelhorn SE, Fitting D, Mihm U, Susser S, et al. (2013) Deep sequencing reveals mutagenic effects of ribavirin during monotherapy of hepatitis C virus genotype 1-infected patients. J Virol 87: 6172-6181.
11. Ortega-Prieto AM, Sheldon J, Grande-Perez A, Tejero H, Gregori J, et al. (2013) Extinction of hepatitis C virus by ribavirin in hepatoma cells involves lethal mutagenesis. PLoS One 8: e71039.
12. Steinmann E, Brohm C, Kallis S, Bartenschlager R, Pietschmann T (2008) Efficient trans-encapsidation of hepatitis C virus RNAs into infectious virus-like particles. J Virol 82: 7034-7046.
13. Mingorance L, Castro V, Avila-Perez G, Calvo G, Rodriguez MJ, et al. (2018) Host phosphatidic acid phosphatase lipin1 is rate limiting for functional hepatitis C virus replicase complex formation. PLoS Pathog 14: e1007284.
14. Perales C, Beach NM, Gallego I, Soria ME, Quer J, et al. (2013) Response of hepatitis C virus to long-term passage in the presence of alpha interferon: multiple mutations and a common phenotype. J Virol 87: 7593-7607.
15. Gallego I, Gregori J, Soria ME, Garcia-Crespo C, Garcia-Alvarez M, et al. (2018) Resistance of high fitness hepatitis C virus to lethal mutagenesis. Virology 523: 100-109.
16. Gallego I, Sheldon J, Moreno E, Gregori J, Quer J, et al. (2016) Barrier-Independent, Fitness-Associated Differences in Sofosbuvir Efficacy against Hepatitis C Virus. Antimicrob Agents Chemother 60: 3786-3793.
17. Sheldon J, Beach NM, Moreno E, Gallego I, Pineiro D, et al. (2014) Increased replicative fitness can lead to decreased drug sensitivity of hepatitis C virus. J Virol 88: 12098-12111.
18. Geller R, Estada U, Peris JB, Andreu I, Bou JV, et al. (2016) Highly heterogeneous mutation rates in the hepatitis C virus genome. Nat Microbiol 1: 16045.
19. Moreno E, Gallego I, Gregori J, Lucia-Sanz A, Soria ME, et al. (2017) Internal Disequilibria and Phenotypic Diversification during Replication of Hepatitis C Virus in a Noncoevolving Cellular Environment. J Virol 91: pii: e02505-02516.

20. Ranjith-Kumar CT, Gutshall L, Kim MJ, Sarisky RT, Kao CC (2002) Requirements for de novo initiation of RNA synthesis by recombinant flaviviral RNA-dependent RNA polymerases. J Virol 76: 12526-12536.
21. Ranjith-Kumar CT, Kim YC, Gutshall L, Silverman C, Khandekar S, et al. (2002) Mechanism of de novo initiation by the hepatitis C virus RNA-dependent RNA polymerase: role of divalent metals. J Virol 76: 12513-12525.
22. Cai Z, Yi M, Zhang C, Luo G (2005) Mutagenesis analysis of the rGTP-specific binding site of hepatitis C virus RNA-dependent RNA polymerase. J Virol 79: 11607-11617.
23. Chinnaswamy S, Murali A, Li P, Fujisaki K, Kao CC (2010) Regulation of de novo-initiated RNA synthesis in hepatitis C virus RNA-dependent RNA polymerase by intermolecular interactions. J Virol 84: 5923-5935.
24. Lebsir N, Goueslain L, Farhat R, Callens N, Dubuisson J, et al. (2019) Functional and Physical Interaction between the Arf Activator GBF1 and Hepatitis C Virus NS3 Protein. J Virol 93.
25. Otto GA, Puglisi JD (2004) The pathway of HCV IRES-mediated translation initiation. Cell 119: 369-380.
26. Zona L, Lupberger J, Sidahmed-Adrar N, Thumann C, Harris HJ, et al. (2013) HRas signal transduction promotes hepatitis C virus cell entry by triggering assembly of the host tetraspanin receptor complex. Cell Host Microbe 13: 302-313.
27. Salloum S, Wang H, Ferguson C, Parton RG, Tai AW (2013) Rab18 binds to hepatitis C virus NS5A and promotes interaction between sites of viral replication and lipid droplets. PLoS Pathog 9: e1003513.
28. Cifuentes Kottkamp A, De Jesus E, Grande R, Brown JA, Jacobs AR, et al. (2019) Atovaquone Inhibits Arbovirus Replication through the Depletion of Intracellular Nucleotides. J Virol 93.
29. Ando T, Imamura H, Suzuki R, Aizaki H, Watanabe T, et al. (2012) Visualization and measurement of ATP levels in living cells replicating hepatitis C virus genome RNA. PLoS Pathog 8: e1002561.
30. Mankouri J, Tedbury PR, Gretton S, Hughes ME, Griffin SD, et al. (2010) Enhanced hepatitis C virus genome replication and lipid accumulation mediated by inhibition of AMP-activated protein kinase. Proc Natl Acad Sci U S A 107: 11549-11554.
31. Ross FA, Jensen TE, Hardie DG (2016) Differential regulation by AMP and ADP of AMPK complexes containing different gamma subunit isoforms. Biochem J 473: 189-199.
32. Xiao B, Sanders MJ, Underwood E, Heath R, Mayer FV, et al. (2011) Structure of mammalian AMPK and its regulation by ADP. Nature 472: 230-233.
33. Rena G, Hardie DG, Pearson ER (2017) The mechanisms of action of metformin. Diabetologia 60: 1577-1585.
34. Huang H, Kang R, Wang J, Luo G, Yang W, et al. (2013) Hepatitis C virus inhibits AKT-tuberous sclerosis complex (TSC), the mechanistic target of rapamycin (MTOR) pathway, through endoplasmic reticulum stress to induce autophagy. Autophagy 9: 175-195.
35. Vignuzzi M, Lopez CB (2019) Defective viral genomes are key drivers of the virus-host interaction. Nat Microbiol 4: 1075-1087.
36. Sabo DL, Domingo E, Bandle EF, Flavell RA, Weissmann C (1977) A guanosine to adenosine transition in the 3' terminal extracistronic region of bacteriophage Q beta RNA leading to loss of infectivity. J Mol Biol 112: 235-252.
37. Davis AR, Hiti AL, Nayak DP (1980) Influenza defective interfering viral RNA is formed by internal deletion of genomic RNA. Proc Natl Acad Sci U S A 77: 215-219.
38. Nomoto A, Jacobson A, Lee YF, Dunn J, Wimmer E (1979) Defective interfering particles of poliovirus: mapping of the deletion and evidence that the deletions in the genomes of DI(1), (2) and (3) are located in the same region. J Mol Biol 128: 179-196.

581 39. O'Hara PJ, Nichol ST, Horodyski FM, Holland JJ (1984) Vesicular stomatitis virus defective
582 interfering particles can contain extensive genomic sequence rearrangements and
583 base substitutions. Cell 36: 915-924.
584 40. Holland JJ, Villarreal LP (1974) Persistent noncytocidal vesicular stomatitis virus infections
585 mediated by defective T particles that suppress virion transcriptase. Proc Natl Acad Sci
586 U S A 71: 2956-2960.
587 41. Kirkegaard K, Baltimore D (1986) The mechanism of RNA recombination in poliovirus. Cell
588 47: 433-443.
589 42. Arnold JJ, Cameron CE (1999) Poliovirus RNA-dependent RNA polymerase (3Dpol) is
590 sufficient for template switching in vitro. J Biol Chem 274: 2706-2716.
591 43. Roux L, Simon AE, Holland JJ (1991) Effects of defective interfering viruses on virus
592 replication and pathogenesis in vitro and in vivo. Adv Virus Res 40: 181-211.
593 44. Grande-Perez A, Lazaro E, Lowenstein P, Domingo E, Manrubia SC (2005) Suppression of
594 viral infectivity through lethal defection. Proc Natl Acad Sci U S A 102: 4448-4452.
595 45. Martin V, Abia D, Domingo E, Grande-Perez A (2010) An interfering activity against
596 lymphocytic choriomeningitis virus replication associated with enhanced mutagenesis.
597 J Gen Virol 91: 990-1003.
598 46. Mims CA (1956) Rift Valley Fever virus in mice. IV. Incomplete virus; its production and
599 properties. Br J Exp Pathol 37: 129-143.
600 47. Cave DR, Hendrickson FM, Huang AS (1985) Defective interfering virus particles modulate
601 virulence. J Virol 55: 366-373.
602 48. Santak M, Markusic M, Balija ML, Kopac SK, Jug R, et al. (2015) Accumulation of defective
603 interfering viral particles in only a few passages in Vero cells attenuates mumps virus
604 neurovirulence. Microbes Infect 17: 228-236.
605 49. Bernardin F, Stramer SL, Rehermann B, Page-Shafer K, Cooper S, et al. (2007) High levels of
606 subgenomic HCV plasma RNA in immunosilent infections. Virology 365: 446-456.
607 50. Cheroni C, Donnici L, Aghemo A, Balistreri F, Bianco A, et al. (2015) Hepatitis C Virus
608 Deletion Mutants Are Found in Individuals Chronically Infected with Genotype 1
609 Hepatitis C Virus in Association with Age, High Viral Load and Liver Inflammatory
610 Activity. PLoS One 10: e0138546.
611 51. Karamichali E, Chihab H, Kakkanas A, Marchio A, Karamitros T, et al. (2018) HCV Defective
612 Genomes Promote Persistent Infection by Modulating the Viral Life Cycle. Front
613 Microbiol 9: 2942.
614 52. Noppornpanth S, Smits SL, Lien TX, Poovorawan Y, Osterhaus AD, et al. (2007)
615 Characterization of hepatitis C virus deletion mutants circulating in chronically infected
616 patients. J Virol 81: 12496-12503.
617 53. Pacini L, Graziani R, Bartholomew L, De Francesco R, Paonessa G (2009) Naturally occurring
618 hepatitis C virus subgenomic deletion mutants replicate efficiently in Huh-7 cells and
619 are trans-packaged in vitro to generate infectious defective particles. J Virol 83: 9079-
620 9093.
621 54. Lopez-Jimenez AJ, Clemente-Casares P, Sabariegos R, Llanos-Valero M, Bellon-Echeverria I,
622 et al. (2014) Hepatitis C virus polymerase-polymerase contact interface: significance
623 for virus replication and antiviral design. Antiviral Res 108: 14-24.
624 55. Marukian S, Jones CT, Andrus L, Evans MJ, Ritola KD, et al. (2008) Cell culture-produced
625 hepatitis C virus does not infect peripheral blood mononuclear cells. Hepatology 48:
626 1843-1850.
627 56. Agudo R, Ferrer-Orta C, Arias A, de la Higuera I, Perales C, et al. (2010) A multi-step process
628 of viral adaptation to a mutagenic nucleoside analogue by modulation of transition
629 types leads to extinction-escape. PLoS Pathog 6: e1001072.
630 57. Sanchez G, Bosch A, Gomez-Mariano G, Domingo E, Pinto RM (2003) Evidence for
631 quasispecies distributions in the human hepatitis A virus genome. Virology 315: 34-42.

632 58. Clemente-Casares P, Lopez-Jimenez AJ, Bellon-Echeverria I, Encinar JA, Martinez-Alfaro E,
633 et al. (2011) De novo polymerase activity and oligomerization of hepatitis C virus RNA-
634 dependent RNA-polymerases from genotypes 1 to 5. PLoS One 6: e18515.
635 59. Vo NV, Tuler JR, Lai MM (2004) Enzymatic characterization of the full-length and C-
636 terminally truncated hepatitis C virus RNA polymerases: function of the last 21 amino
637 acids of the C terminus in template binding and RNA synthesis. Biochemistry 43:
638 10579-10591.
639 60. Doskey CM, van 't Erve TJ, Wagner BA, Buettner GR (2015) Moles of a Substance per Cell Is
640 a Highly Informative Dosing Metric in Cell Culture. PLoS One 10: e0132572.

641

642

643 **Table 1.** Effects of nucleosides on cell viability and HCV replication. CC_{50}, IC_{50}, and
644 therapeutic index (TI, CC_{50}/IC_{50}) values are shown for Adenosine (Ade), Cytosine (Cyt),
645 Guanosine (Gua), and Uridine (Uri) in Huh-7.5 reporter cells.

	CC_{50} (μM)	IC_{50} (μM)	TI
Ade	641 ± 40	108 ± 7	5.9
Cit	> 800	> 800	n.d.
Gua	> 800	164 ± 2.4	≥ 4.9
Uri	> 800	> 800	n.d.

646

647

Table 2. Effects of nucleosides on BHK-21 cells viability and VSV, FMDV, and LCMV replication. CC_{50}, IC_{50}, and therapeutic index (TI, CC_{50}/IC_{50}) values are shown for Adenosine (Ade), Cytosine (Cit), Guanosine (Gua), and Uridine (Uri) in BHK-21 cells.

		IC_{50} (μM) (TI)		
	CC_{50} (μM)	VSV	FMDV	LCMV
Ade	391 ± 68	650 ± 105.4 (0.6)	> 800 (n.d.)	213 ± 56.2 (1.8)
Cit	> 800	> 800 (n.d.)	> 800 (n.d.)	566.4 ± 216.7 (≥ 1.4)
Gua	> 800	734 ± 59.4 (≤ 1.1)	> 800 (n.d.)	348 ± 36 (≥ 2.3)
Uri	> 800	> 800 (n.d.)	> 800 (n.d.)	157.8 ± 7.6 (≥ 5.1)

n.d. Not Determined.

Table 3. Mutant spectrum analysis of the hepatitis C virus populations passaged in the absence and presence of guanosine (Gua)

HCV population[a]	N. of nucleotides analyzed (clones/haplotypes)[b]	N. of different (total) mutations[c]	Mutation frequency	
			Minimum[d]	Maximum[e]
HCV p0, [no drug] p3	28,208 (53/21)	23 (25)	8.2×10^{-4}	8.9×10^{-4}
HCV p0, [Gua 500 μM] p3	33,339 (64/34)	45 (79)	1.4×10^{-3}	2.4×10^{-3}
HCV p0, [Gua 800 μM] p3	35,606 (68/30)	32 (59)	9.0×10^{-4}	1.7×10^{-3}

[a]The populations analyzed are those schematically represented in Fig 1, and their origin is detailed in Materials and Methods; [no drug] means passages in absence of drug; [Gua 500 μM] means passages in the presence of 500 μM guanosine; [Gua 800 μM] means passages in the presence of 800 μM guanosine; p indicates passage number.

[b]The genomic region analyzed by molecular cloning-Sanger sequencing spans residues 6220 to 6758 of the NS4B- and NS5A-coding region; the residue numbering corresponds to the JFH-1 genome (GenBank accession number #AB047639). The values in parenthesis indicate the number of clones analyzed followed by the number of haplotypes (number of different RNA sequences) found in the mutant spectrum.

[c]Number of different and total mutations identified by comparing the sequence of each individual clone with the consensus sequence of the corresponding population.

[d]Data represent the average number of different mutations (counted relative to the consensus sequence of the corresponding population) per nucleotide in the components of the mutant spectrum. The statistical significance of the differences between two populations (χ^2 test) is the following: HCV p0, [no drug] p3 versus HCV p0, [Gua 500 μM] p3: $p = 0.0622$; HCV p0, [no drug] p3 versus HCV p0, [Gua 800 μM] p3: $p = 0.8257$; HCV p0, [Gua 500 μM] p3 versus HCV p0, [Gua 800 μM] p3: $p = 0.0977$.

[e]Data represent the average number of total mutations (counted relative to the consensus sequence of the corresponding population) per nucleotide in the components of the mutant spectrum relative to the consensus sequence of the corresponding population. The statistical significance of the differences between two populations (proportion test) is the following: HCV p0, [no drug] p3 versus HCV p0, [Gua 500 μM] p3: $p < 0.0001$; HCV p0, [no drug] p3 versus HCV p0, [Gua 800 μM] p3: $p = 0.0107$; HCV p0, [Gua 500 μM] p3 versus HCV p0, [Gua 800 μM] p3: $p = 0.0452$

680 **Table 4.** Indels found in the mutant spectra of HCV p0 after 3 passages in the absence
681 and presence of Gua 500 µM and 800 µM.

682

HCV population[a]	Indel	Position[c]	Number of deleted or inserted nucleotides	Region	Premature STOP position	# of clones
HCV p0, no Gua p3	-	0	-	-	-	
HCV p0, [Gua 500 µM] p3	**Deletion 1**	6220	1	NS4B	6243	2
	Deletion 2[b]	6278-6287	10	NS5A	6315	4
	Deletion 3[b]	6289-6292	4	NS5A	6315	4
	Deletion 4[b]	6294-6296	3	NS5A	6315	4
	Deletion 5[b]	6298-6300	3	NS5A	6315	4
	Deletion 6	6659-6704	46	NS5A	6864	1
	Deletion 7	6744	1	NS5A	6864	1
	Deletion 8	6751	1	NS5A	6864	1
	Deletion 9	6753-6756	4	NS5A	6864	1
	Deletion 10	6757	1	NS5A	6864	1
	Insertion 1	6225	1	NS4B	6246	1
	Insertion 2	6301	1	NS5A	6298	1
HCV p0, [Gua 800 µM] p3	**Deletion 1**	6220	1	NS4B	6243	13
	Deletion 2	6231	1	NS4B	6243	1
	Deletion 3	6748	1	NS5A	6864	3
	Deletion 4	6749	1	NS5A	6864	1
	Deletion 5	6757	1	NS5A	6864	2

683 [a]The populations analyzed are those schematically represented in Fig 1, and their origin
684 is detailed in Materials and Methods; [Gua 500 µM] means passages in the presence of
685 500 µM guanosine; [Gua 800 µM] means passages in the presence of 800 µM
686 guanosine; p indicates passage number.

687 [b]Deletions 2, 3, 4 and 5 were found always together

688 [c]The genomic region analyzed by molecular cloning-Sanger sequencing spans residues
689 6220 to 6758 of the NS4B- and NS5A-coding region; the residue numbering
690 corresponds to the JFH-1 genome (GenBank accession number #AB047639).

691

692 **FIGURE LEGENDS.**

693 **Figure 1. Effect of ribonucleosides on HCV replication. (A)** and **(B)** Effect of guanosine
694 (Gua) on HCV p0 replication. Infectious progeny obtained in the presence of Gua 500 μM (A)
695 and Gua 800 μM (B); four replicas for each condition are shown (red squares). HCV p0 titer in
696 the absence of treatment (black circles) and values for a HCV lethal mutant GNN (black
697 crosses) are also shown (see Methods). **(C)** and **(D)** Effect of adenosine (Ade, blue squares),
698 cytosine (Cyt, green squares), and uridine (Uri, orange squares) on HCV p0 replication.
699 Infectious progeny obtained in the presence of the corresponding nucleoside at 500 μM (C) and
700 at 800 μM (D). HCV p0 viral titer in the absence of treatment (black circles) and values for a
701 HCV lethal mutant GNN (black crosses) are also shown. **(E)** HCV p100 viral titer in the
702 absence (black circles) or presence of Gua 500 μM (yellow symbols), and Gua 800 μM (red
703 symbols). Two replicates are shown for each condition in presence of nucleosides. The
704 discontinuous horizontal line marks the limit of detection of virus infectivity. Procedures for
705 serial infections and titration of infectivity are detailed in Materials and Methods.

706 **Figure 2. Treatment with Gua causes a reduction in the efficiency of early aspects of the**
707 **infection. (A)** Impact of nucleoside treatment on single cycle trans-complemented HCV
708 particles (HCVtcp) infection efficiency. Huh-7 cells were pre-treated with the indicated doses of
709 nucleoside for 20 hours before inoculation with HCVtcp in the presence or absence of the
710 nucleosides. As a positive inhibition control, target cells were treated with the entry inhibitor
711 hydroxyzine (HDH) at the time of infection (5μM). Single cycle infection efficiency was
712 determined by measuring luciferase activity in total cell extracts 48 hours post-inoculation. **(B)**
713 Huh-7 cells were pre-treated with the indicated doses of nucleoside for 20 hours before
714 transfection with in vitro-transcribed subgenomic viral RNA-containing liposomes in the
715 presence or absence of the nucleosides. As a positive inhibition control, target cells were treated
716 with the replication inhibitor 2´-c-methyladenosine (2mAde) (10 μM). Primary translation (5
717 hours) and RNA replication efficiency (24 and 48 hours) was determined by measuring
718 luciferase activity in total cell extracts at different times post-transfection. Data are shown as

719 average and standard deviation of two experiments performed in triplicate (N=6). Significance
720 (Student's T-test): ***p<0.0005; *p<0.05.

721 **Figure 3. Effect of nucleosides on FMDV, LCMV and VSV replication.** Effect of adenosine
722 (Ade), cytidine (Cyt), uridine (Uri), and guanosine (Gua) on the production of infectious
723 progeny of FMDV **(A)**, LCMV **(B)** and VSV **(C)** in BHK-21 cells at an initial m.o.i. of 0.05
724 $TCID_{50}$ per cell, in the absence (C-) or presence of 800 μM of the indicated nucleoside.
725 Infectivity was determined at passage 3 in the cell culture supernatant as described in Materials
726 and Methods. **(D)** Comparative inhibition of VSV and HCV p0 progeny production in Huh-7.5
727 reporter cells in the presence of 800 μM Gua. The titer shown for HCV is the average (four
728 replicas) of titers determined at passage 3 in the supernatants of the serial infections
729 (corresponding to Fig 1). Procedures for serial infections and titration of infectivity are detailed
730 in Materials and Methods. Significance (Student's T-test): ** $p < 0.005$.

731

732 **Figure 4. Effect of Gua on NS5BΔ21 RNA polymerase activity. (A)** Recombinant HCV
733 NS5BΔ21 polymerase was added to a reaction containing a 540-nt RNA template [18], the four
734 nucleoside-triphosphates (ATP, CTP, GTP, and UTP) and the indicated concentrations of Gua.
735 Product quantification from three replicates (average ± SEM) and a representative experiment
736 (below) are shown. Polymerase activity is normalized with respect to its maximum activity. The
737 band indicates a new synthesis RNA product of 540 nt length. **(B)** A representative experiment
738 as in A, but using the 19-nt LE19 RNA as a template. DN, PE, and TS indicate reaction
739 products of *de novo* synthesis, primer extension, and template switching, respectively [54].
740 Procedures are detailed in Materials and Methods. Significance (Student's T-test): ** $p < 0.005$.

741

742 **Figure 5. Effect of Gua on intracellular nucleotides.** Effect of treatment of Huh-7.5 cells with
743 Gua on the level of intracellular nucleoside-triphosphates (**A**) and intracellular nucleoside-
744 diphosphates (**B**). Data are represented as a box and whisker chart showing distribution of data
745 into quartiles, highlighting the mean and outliers. Error lines indicate variability outside the

upper and lower quartiles. Data points (red circles) are grouped in black (no treatment), orange (500 μM Gua) and blue (800 μM Gua) boxes. Significance (Student's T-test): * $p < 0.05$; ** $p < 0.005$; *** $p < 0.0005$. The table shows the p-value and the fold of difference between treatment conditions for each nucleoside di- and triphosphate.

Figure 6. Effect of nucleoside-triphosphate concentration on NS5BΔ21 RNA polymerase activity. (**A)** Polyacrylamide gel showing the products for de novo (DN), primer extension (PE) and template switching (TS) obtained with HCV NS5BΔ21 at increasing concentrations (100, 500, 800, and 1000 μM) of UTP in the presence of radiolabeled α^{32}P-CTP. ATP and GTP concentrations were maintained at 100 μM and 500 μM, respectively (left panel). Graphic representation of densitometric values obtained from the electropherogram shown in A (red diamonds, yellow triangles, and black squares correspond to *de novo* (DN), primer extension (PE), and template switching (TS) activities, respectively) (right panel). **(B)** Corresponds to experiments as in **A** but for increasing concentrations of ATP, with UTP and GTP maintained at 100 μM and 500 μM, respectively. **(C)** Corresponds to experiments as in **A** but for increasing concentrations of GTP, with ATP and UTP both maintained at 100 μM. Activities were normalized to their maximum values. Densitometric data represent the mean of at least three independent experiments. Error bars correspond to standard error of the mean. Horizontal lines indicate statistically significant differences (Student's T-test) between the activity values that link, using the same color code as the activity type. Details of the activity measurements are given in Materials and Methods. Significance (Student's T-test): *** $p < 0.0005$, ** $p < 0.005$, * $p < 0.05$.

Figure 7. Effect of NDPs on NS5BΔ21 RNA polymerase activity. (A) Polyacrylamide gel showing the products for *de novo* (DN), primer extension (PE) and template switching (TS) obtained with HCV NS5BΔ21 at increasing concentrations (0, 166, 333, 500, 800, and 1000 μM) of UDP in the presence of ATP and UTP at a final concentration of 100 μM, GTP at 500

773 μM, and radiolabeled α^{32}P-CTP (left panel). Graphic representation of densitometric values
774 obtained from the electropherogram shown in A (red diamonds, yellow triangles, and black
775 squares correspond to *de novo* (DN), primer extension (PE), and template switching (TS)
776 activities, respectively) (right panel). **(B)** Corresponds to experiments as in **A** but for increasing
777 concentrations of ADP. **(C)** corresponds to experiments as in **A** but for increasing
778 concentrations of GDP. Activities were normalized to their maximum values. Densitometric
779 data represent the mean of at least three independent experiments. Error bars correspond to
780 standard error of the mean. Horizontal lines indicate statistically significant differences
781 (Student's T-test) between activity values, using the same color code as the activity type.
782 Details of the activity measurements are given in Materials and Methods. Significance
783 (Student's T-test): ** $p < 0.005$, * $p < 0.05$.

784

785 **Figure 8.** Effect of guanosine on HCV specific infectivity. Huh-7.5 reporter cells were infected
786 with HCVp0 at an initial m.o.i. of 0.05 TCID50/cell, in the absence or presence of Gua at the
787 indicated concentrations. HCV GNN infection was used as a negative control. **(A)** Extracellular
788 viral RNA measured by quantitative RT-PCR in different passages. The populations correspond
789 to those of the experiment described in Fig 1 and the values in each passage are the average of
790 the three replicas; standard deviations are given. **(B)** Specific infectivities calculated from the
791 infectivity values of the Fig. 1A and Fig. 1B and the extracellular RNA concentrations indicated
792 in Fig 8A. The horizontal dashed line indicates the limit of detection of viral RNA and specific
793 infectivity. Black, yellow, and red symbols correspond to no drug, Gua 500 μM, and Gua 800
794 μM, respectively. Values for a HCV lethal mutant GNN (black crosses) are also shown. Details
795 of the procedures are given in Materials and Methods. Significance (Student's T-test): ** $p <$
796 0.005, * $p < 0.05$.

797

798 **Figure 9. Indels found in the mutant spectrum of HCV p0 passaged in the presence of**
799 **Gua.** The nucleotide sequence of HCV genomic residues 6220 to 6758 was determined for 53

800 molecular clones derived from the population in absence of Gua, and 132 molecular clones from
801 populations passaged in presence of Gua (data in Table 3). Deduced amino acids (single letter
802 code) are given for residues located at the carboxy-terminal region of NS4B preceding NS5A
803 amino acids. For clarity, only residues around insertions or deletions are shown; three squared
804 points indicate missing amino acids (sequence is that of JFH-1; accession number AB047639).
805 No indels were detected in the population passaged in absence of Gua. (**A**) Deletions in the
806 population passaged in the presence of 500 μM guanosine. Red boxes indicate nucleotides that
807 were deleted in a component of the mutant spectrum, with the deletion size indicated in the
808 filled boxes. (**B**) Insertions in the mutant spectrum of the population passaged in the presence of
809 500 μM Gua are marked with a blue triangle. (C) Deletions found in the HCV populations
810 passaged in the presence of 800 μM Gua. Procedures for HCV genome sequencing are
811 described in Materials and Methods.

812

Figure 1

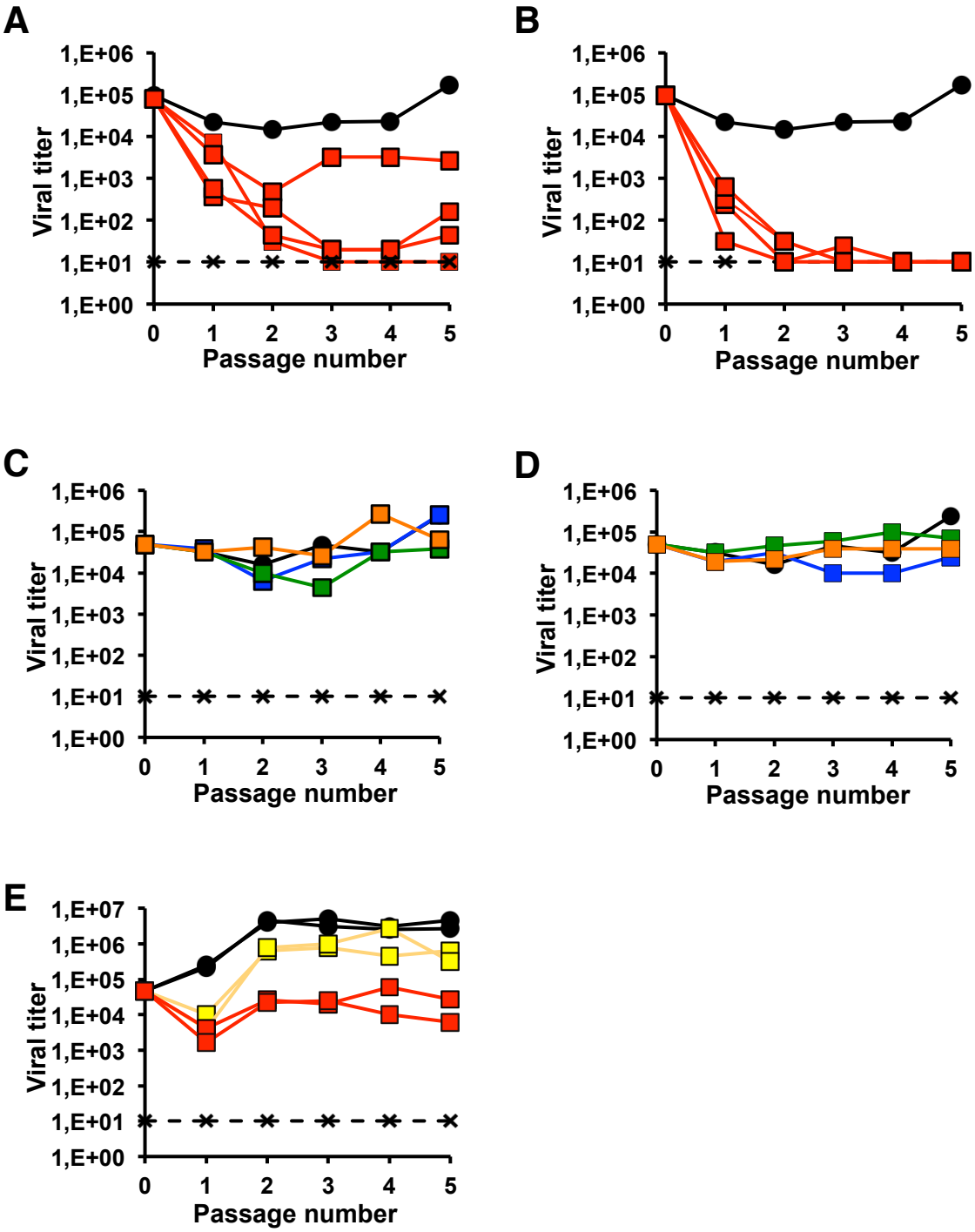
A
B
C
D
E
Viral titer
Passage number
1,E+00
1,E+01
1,E+02
1,E+03
1,E+04
1,E+05
1,E+06
1,E+07
0
1
2
3
4
5

Figure 2

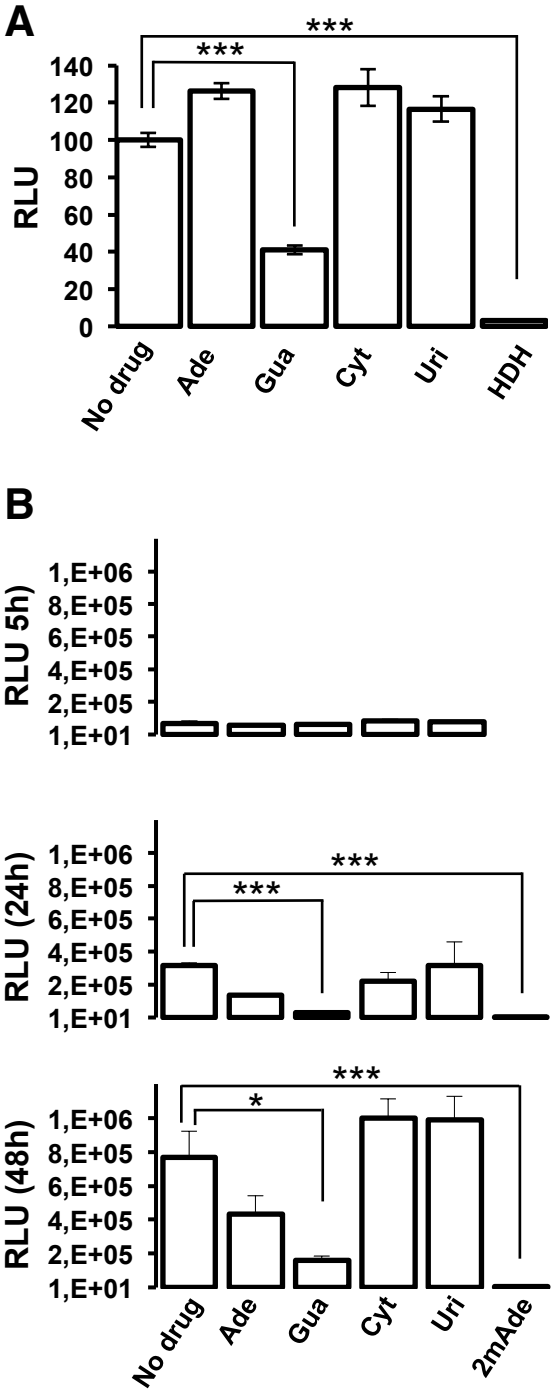
A
***
***
140
120
100
80
60
40
20
0
RLU
No drug
Ade
Gua
Cyt
Uri
HDH
B
RLU 5h)
1,E+06
8,E+05
6,E+05
4,E+05
2,E+05
1,E+01
RLU (24h)
***
***
RLU (48h)
***
*
No drug
Ade
Gua
Cyt
Uri
2mAde

Figure 3

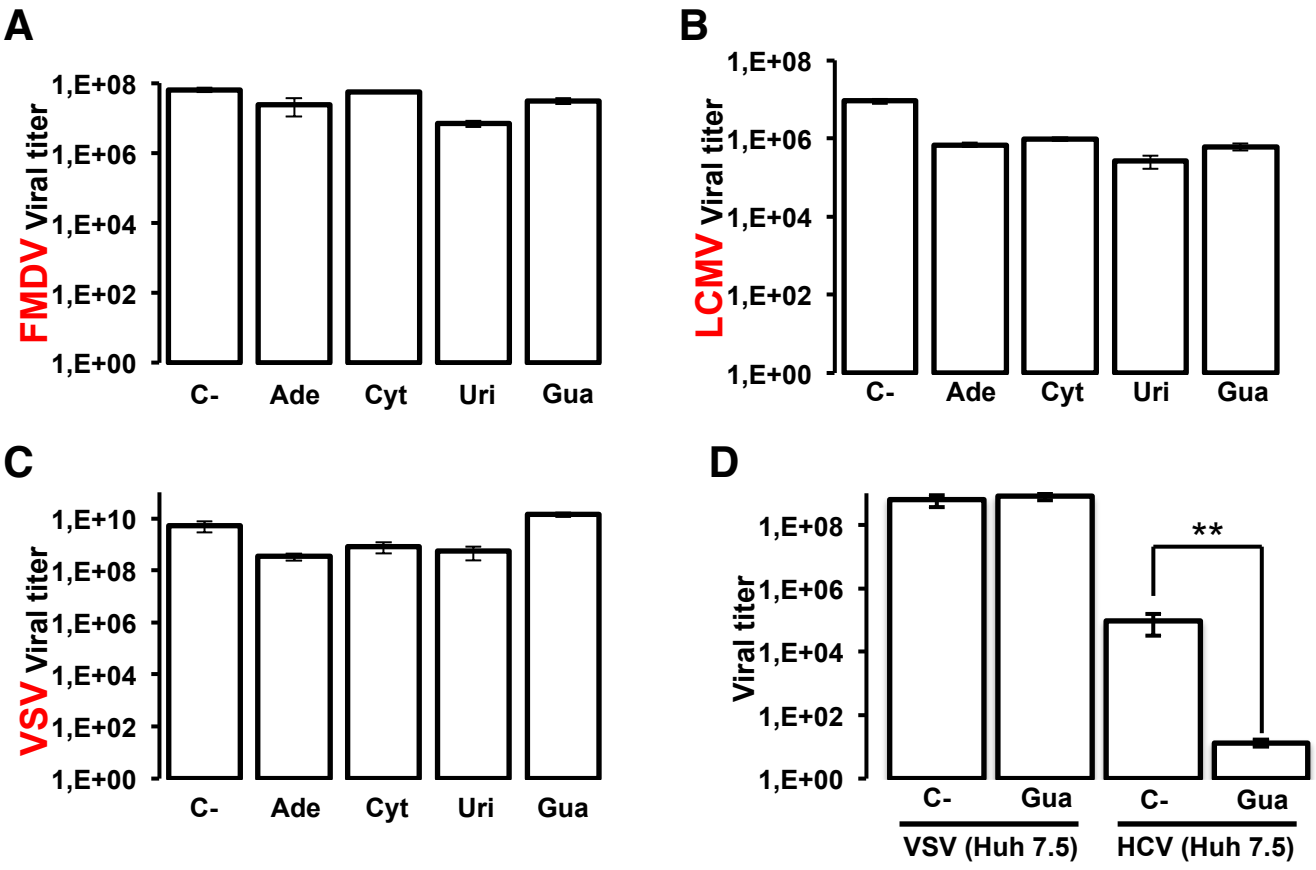
A
FMDV Viral titer
1,E+08
1,E+06
1,E+04
1,E+02
1,E+00
C-
Ade
Cyt
Uri
Gua
B
LCMV Viral titer
1,E+08
1,E+06
1,E+04
1,E+02
1,E+00
C-
Ade
Cyt
Uri
Gua
C
VSV Viral titer
1,E+10
1,E+08
1,E+06
1,E+04
1,E+02
1,E+00
C-
Ade
Cyt
Uri
Gua
D
Viral titer
1,E+08
1,E+06
1,E+04
1,E+02
1,E+00
**
C-
Gua
C-
Gua
VSV (Huh 7.5)
HCV (Huh 7.5)

Figure 4

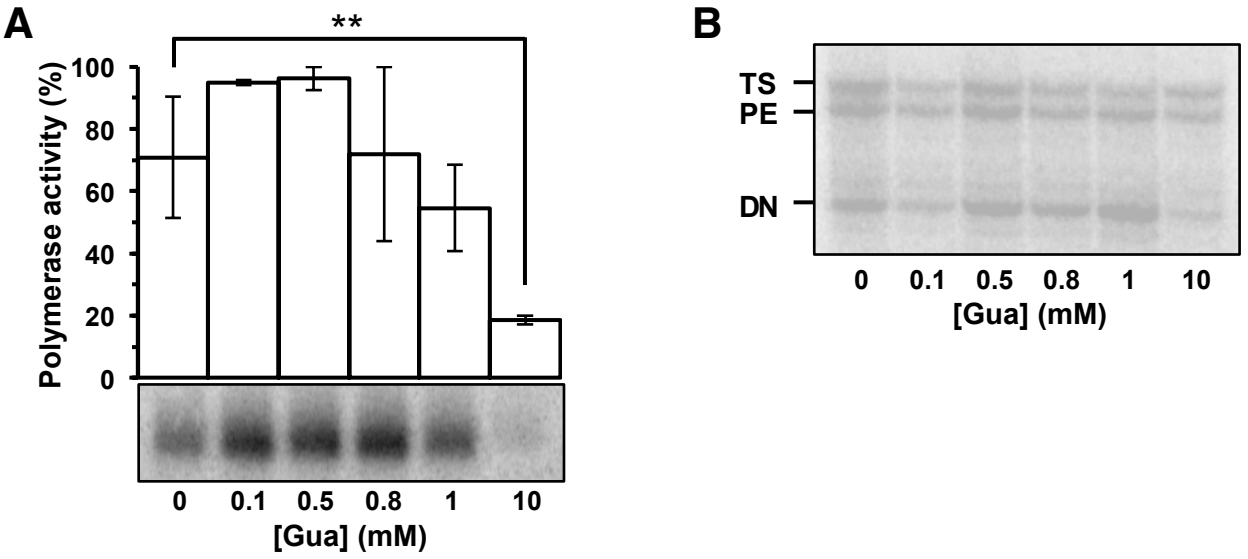
A
**
Polymerase activity (%)
100
80
60
40
20
0
0
0.1
0.5
0.8
1
10
[Gua] (mM)
B
TS
PE
DN
0
0.1
0.5
0.8
1
10
[Gua] (mM)

Figure 5

A

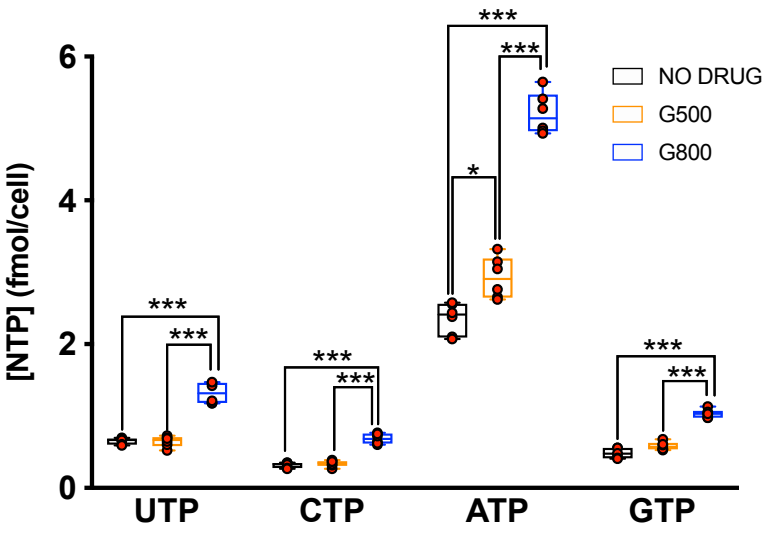

		Guanosine treatment		
		0 vs 500	0 vs 800	500 vs 800
UTP	x-fold	0,9	2	2
	p-value	0,951	0,00026	7,50E-06
CTP	x-fold	1	2,1	2
	p-value	0,484	0,00029	3,10E-06
ATP	x-fold	1,2	2,2	1,8
	p-value	0,027	1,70E-05	2,50E-08
GTP	x-fold	1,2	2,1	1,8
	p-value	0,059	3,70E-05	2,80E-08

B

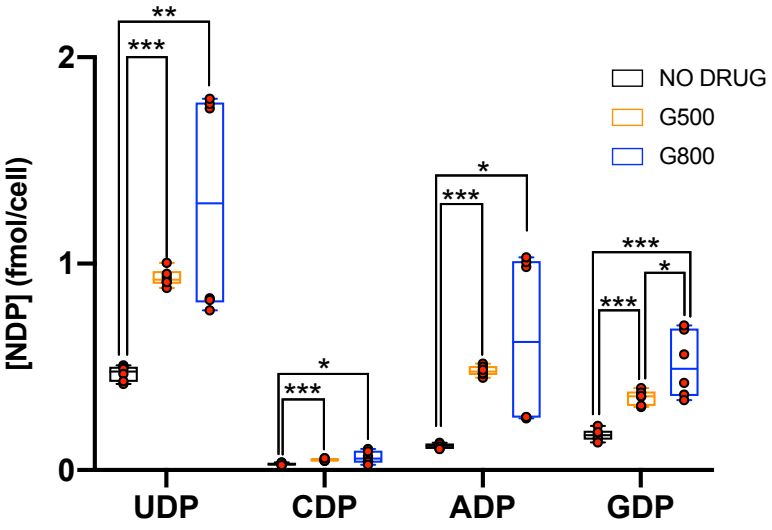

		Guanosine treatment		
		0 vs 500	0 vs 800	500 vs 800
UDP	x-fold	2,0	2,8	1,4
	p-value	1,00E-06	0.0034	0.1
CDP	x-fold	1,7	2,1	1,3
	p-value	3,16E-04	0.027	0.3
ADP	x-fold	4,1	5,4	1,3
	p-value	1,00E-06	0.012	0.39
GDP	x-fold	2,1	3,0	1,5
	p-value	2,00E-06	4,05E-04	0.034

Figure 6

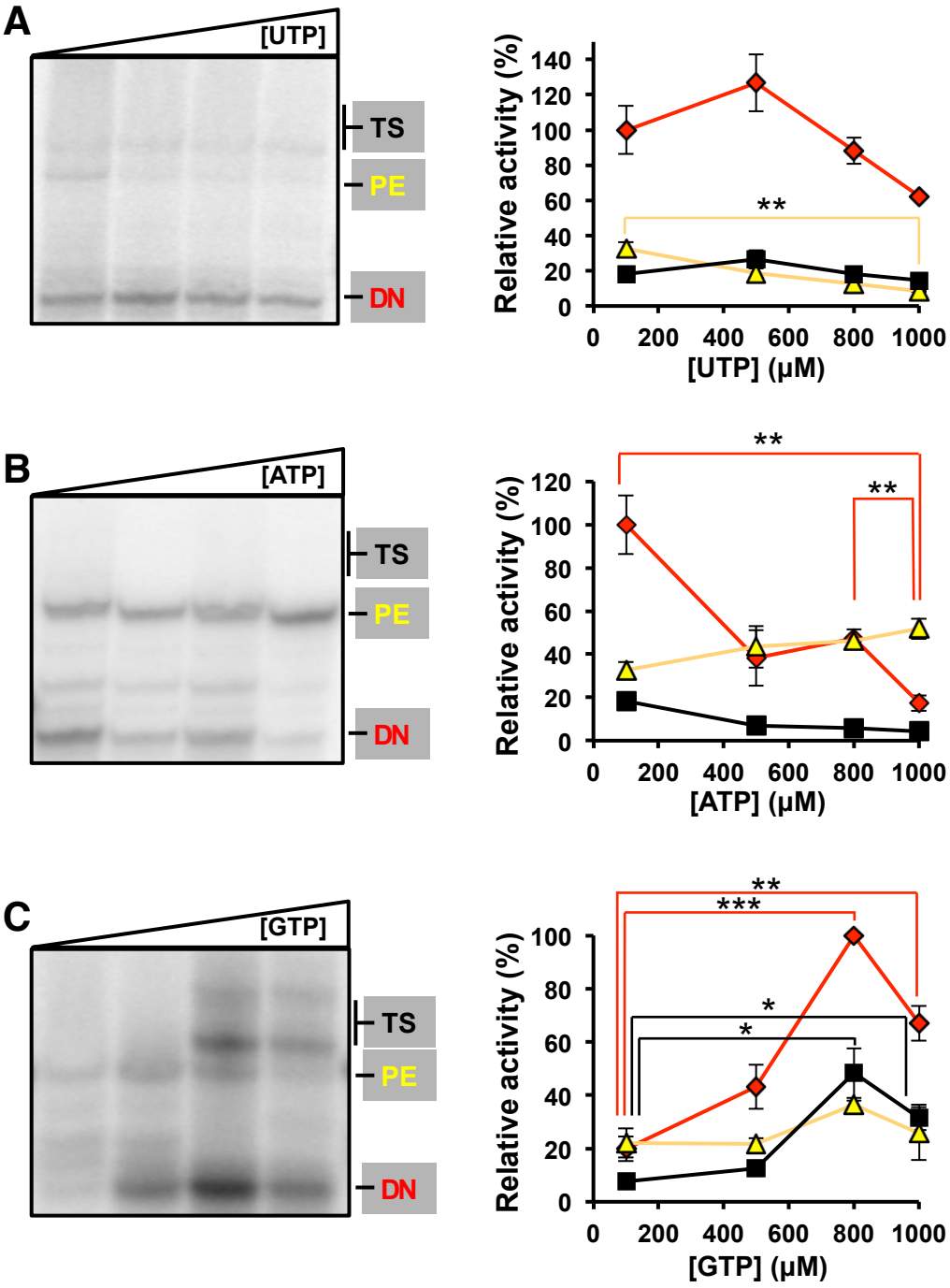
A
[UTP]
TS
PE
DN
Relative activity (%)
140
120
100
80
60
40
20
0
**
0
200
400
600
800
1000
[UTP] (μM)
B
[ATP]
TS
PE
DN
**
**
Relative activity (%)
120
100
80
60
40
20
0
0
200
400
600
800
1000
[ATP] (μM)
C
[GTP]
TS
PE
DN
**
***
*
*
Relative activity (%)
100
80
60
40
20
0
0
200
400
600
800
1000
[GTP] (μM)

Figure 7

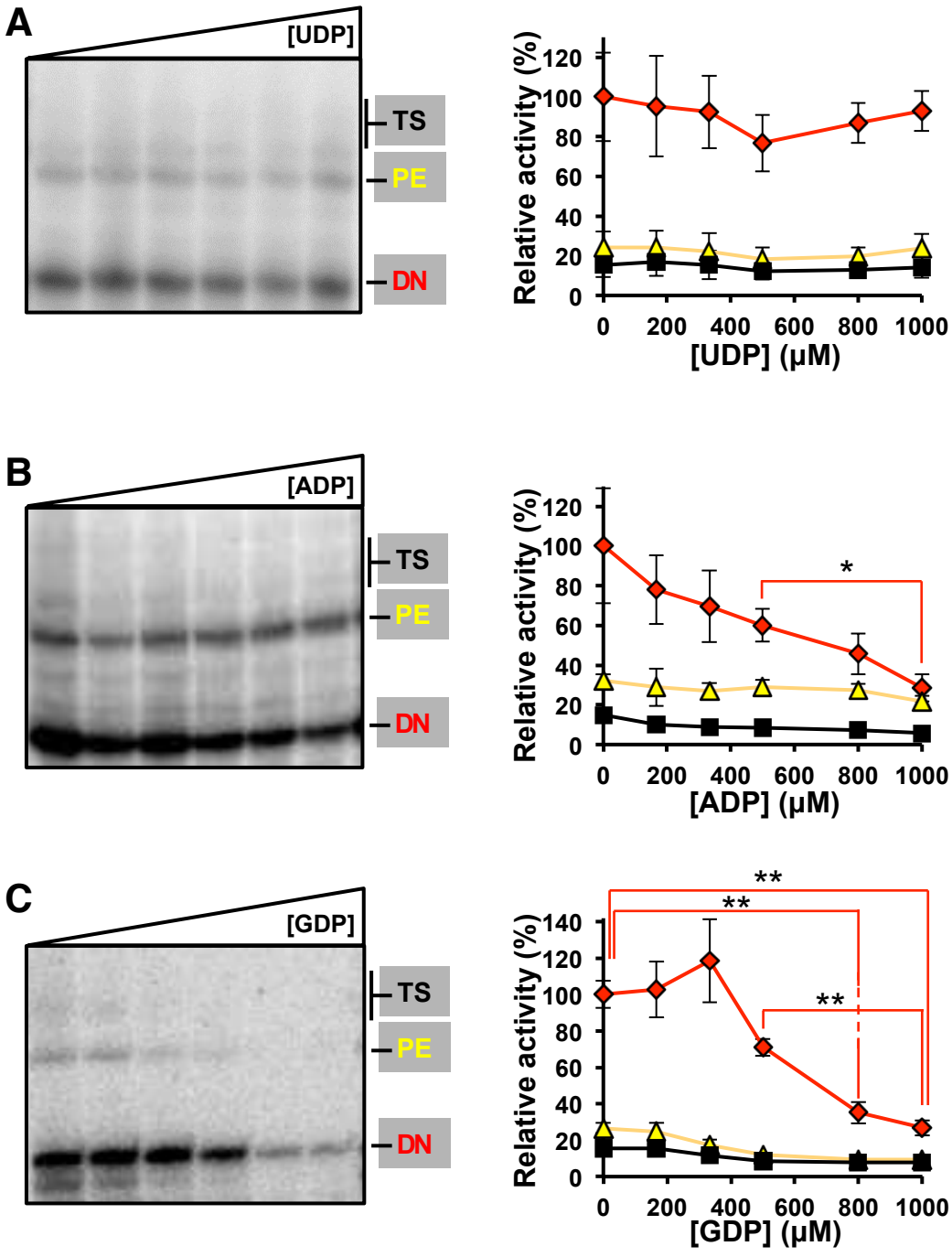
A
[UDP]
TS
PE
DN
Relative activity (%)
120
100
80
60
40
20
0
0
200
400
600
800
1000
[UDP] (μM)
B
[ADP]
TS
PE
DN
*
Relative activity (%)
[ADP] (μM)
C
[GDP]
TS
PE
DN
**
**
**
140
Relative activity (%)
[GDP] (μM)

Figure 8

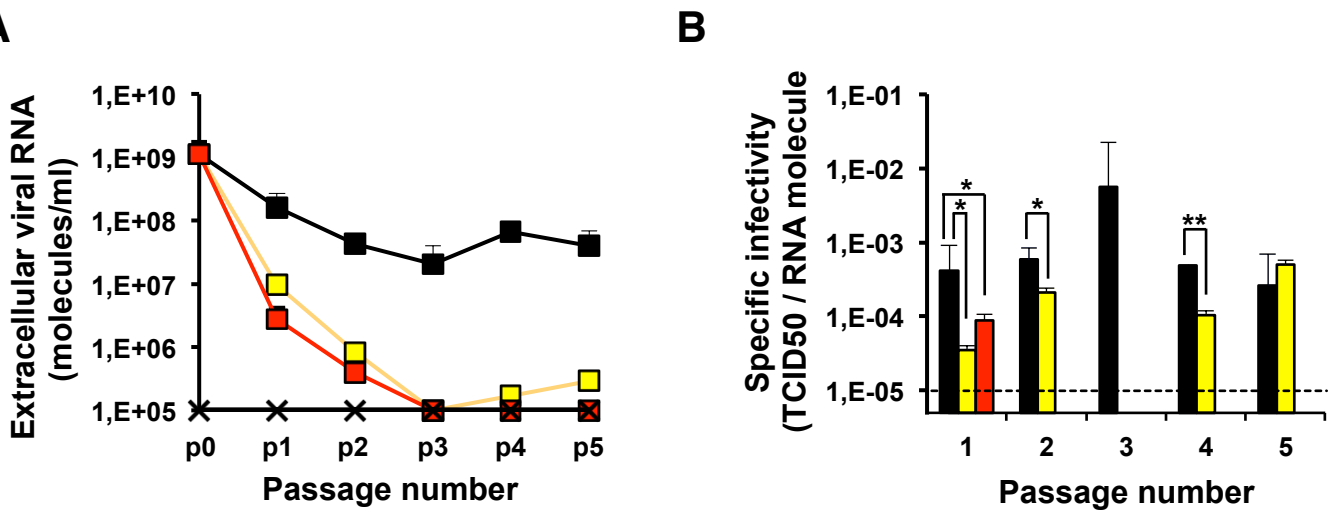
A
Extracellular viral RNA (molecules/ml)
1,E+10
1,E+09
1,E+08
1,E+07
1,E+06
1,E+05
p0
p1
p2
p3
p4
p5
Passage number
B
Specific infectivity (TCID50 / RNA molecule
1,E-01
1,E-02
1,E-03
1,E-04
1,E-05
*
*
*
**
1
2
3
4
5
Passage number

Figure 9

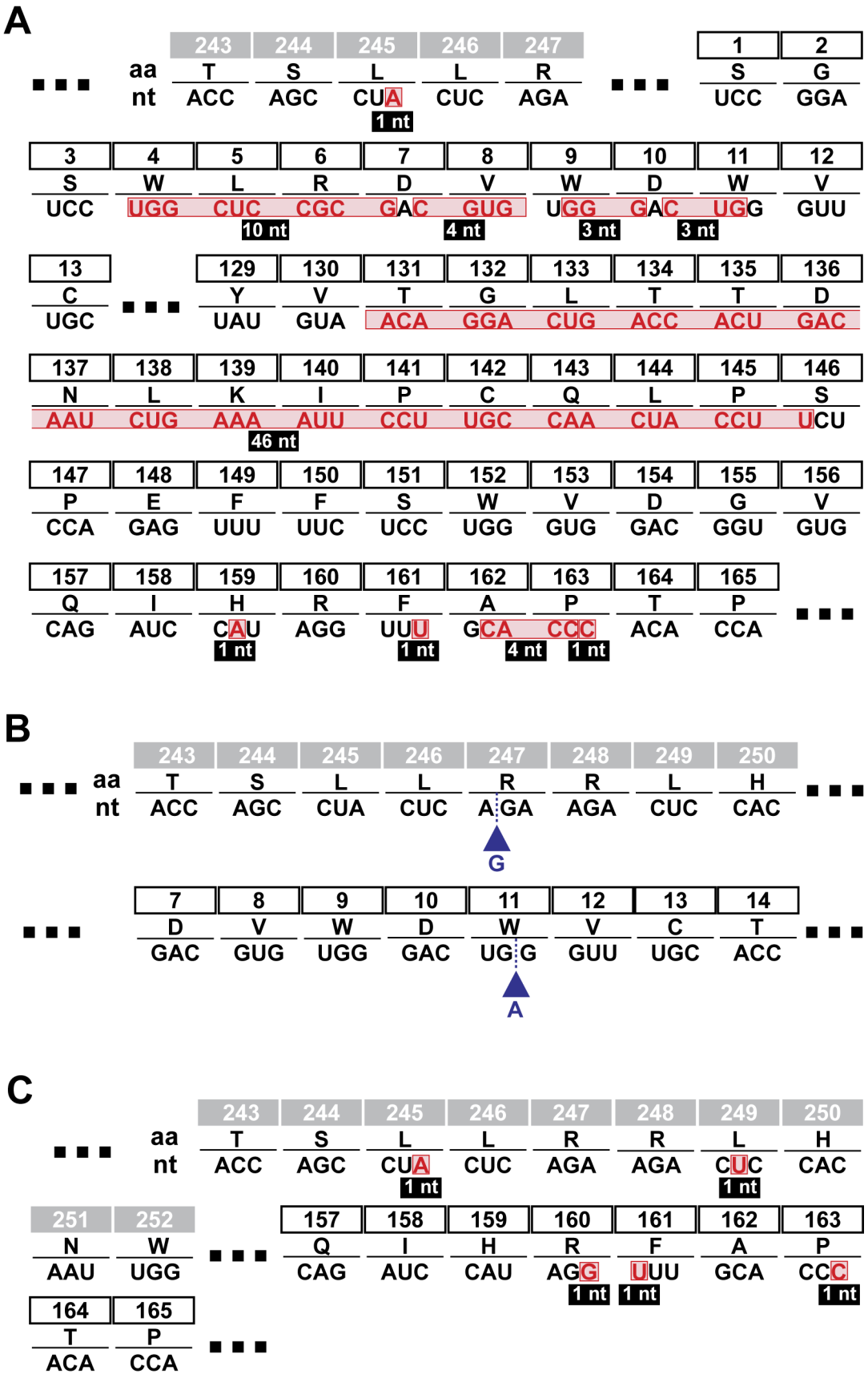
A
aa
nt
243 244 245 246 247
T S L L R
ACC AGC CUA CUC AGA
1 nt
1 2
S G
UCC GGA
3 4 5 6 7 8 9 10 11 12
S W L R D V W D W V
UCC UGG CUC CGC GAC GUG UGG GAC UGG GUU
10 nt 4 nt 3 nt 3 nt
13 129 130 131 132 133 134 135 136
C Y V T G L T T D
UGC UAU GUA ACA GGA CUG ACC ACU GAC
137 138 139 140 141 142 143 144 145 146
N L K I P C Q L P S
AAU CUG AAA AUU CCU UGC CAA CUA CCU UCU
46 nt
147 148 149 150 151 152 153 154 155 156
P E F F S W V D G V
CCA GAG UUU UUC UCC UGG GUG GAC GGU GUG
157 158 159 160 161 162 163 164 165
Q I H R F A P T P
CAG AUC CAU AGG UUU GCA CCC ACA CCA
1 nt 1 nt 4 nt 1 nt
B
aa
nt
243 244 245 246 247 248 249 250
T S L L R R L H
ACC AGC CUA CUC AGA AGA CUC CAC
G
7 8 9 10 11 12 13 14
D V W D W V C T
GAC GUG UGG GAC UGG GUU UGC ACC
A
C
aa
nt
243 244 245 246 247 248 249 250
T S L L R R L H
ACC AGC CUA CUC AGA AGA CUC CAC
1 nt 1 nt
251 252 157 158 159 160 161 162 163
N W Q I H R F A P
AAU UGG CAG AUC CAU AGG UUU GCA CCC
1 nt 1 nt 1 nt
164 165
T P
ACA CCA